



# IMS Technical Program Preview 2016 International Microwave Symposium

MOSCONE CENTER • SAN FRANCISCO, CALIFORNIA, USA  
Symposium Dates: 22-27 MAY 2016 • Exhibition Dates: 24-26 MAY 2016



*GATEWAY TO THE WIRELESS FUTURE*

[IMS2016.org](http://IMS2016.org)



**IEEE**





# Tuesday

# Technical Sessions

13:30-15:10

	Room: 303	Room: 304	Room: 305	Room: 306
	<b>TU3A: Couplers and Dividers</b> Chair: Guoan Wang, <i>University of South Carolina</i> Co-Chair: Banyaner Arigong, <i>Infinion Technologies Americas</i>	<b>TU3B: Wideband Power Amplifiers</b> Chair: Ruediger Quay, <i>Fraunhofer IAF</i> Co-Chair: Arvind Keerti, <i>Qualcomm, Inc.</i>	<b>TU3C: Radio Architectures for Efficient Spectrum Utilization</b> Chair: Ethan Wang, <i>Univ. of California, Los Angeles</i> Co-Chair: Shoichi Narahashi, <i>NTT DoCoMo, Inc.</i>	<b>TU3D: Advances in Terahertz Photonics</b> Chair: Mona Jarrahi, <i>Univ. of California, Los Angeles</i> Co-Chair: Jeffrey Nanzler, <i>Johns Hopkins Univ.</i>
13:30-13:50	<b>TU3A-1: A Planar Filtering Crossover for Three Intersecting Channels</b> Lin-Sheng Wu, <i>Shanghai Jiao Tong University</i> , Junfa Mao, <i>Shanghai Jiao Tong University</i>	<b>TU3B-1: An S-band 240 W Output / 54 % PAE GaN Power Amplifier with Broadband Output Matching Network for both Fundamental and 2nd Harmonic Frequencies</b> Takaaki Yoshioka, <i>Mitsubishi Electric Corporation</i> , Naoki Kosaka, <i>Mitsubishi Electric Corporation</i> , Masatake Hangai, <i>Mitsubishi Electric Corporation</i> , Koji Yamanaka, <i>Mitsubishi Electric Corporation</i>	<b>TU3C-1: RF Spectrum Sensing Receiver System with Improved Frequency Channel Selectivity for Cognitive IoT Sensor Network Applications</b> Jun Gi Hong, <i>Soonchunhyang Univ.</i> , Seok-Jae Lee, <i>Soonchunhyang Univ.</i> , Jongsik Lim, <i>Soonchunhyang Univ.</i> , Won-Sang Yoon, <i>Hoseo Univ.</i> , Sang-Min Han, <i>Soonchunhyang Univ.</i>	<b>TU3D-1: Photonic-based Millimeter and Terahertz Wave Generation Using a Hybrid Integrated Dual DBR Polymer Laser</b> Guillermo Carpintero, <i>Universidad Carlos III De Madrid</i> , Shintaro Hisatake, <i>Osaka Univ.</i> , David De Felipe, <i>Fraunhofer Heinrich Hertz Institute</i> , Robinson Cruzoe Guzman, <i>Universidad Carlos III de Madrid</i> , Tadao Nagatsuma, <i>Osaka Univ.</i> , Norbert KELL, <i>Fraunhofer Heinrich Hertz Institute</i> , Thorsten Göbel, <i>Fraunhofer Heinrich Hertz Institute</i> , Thorsten Göbel, <i>Fraunhofer Heinrich Hertz Institute</i>
13:50-14:10	<b>TU3A-2: A Balanced-to-Balanced Power Divider with Common-Mode Noise Absorption</b> Siang Chen, <i>National Taiwan University</i> , Wei-Chiang Lee, <i>National Taiwan University</i> , Tzong-Lin Wu, <i>National Taiwan University</i>	<b>TU3B-2: A 2-22 GHz Wideband Active Bidirectional Power Divider/Combiner in 130 nm SiGe BiCMOS Technology</b> Ickhyun Song, <i>Georgia Institute of Technology</i> , Moon-Kyu Cho, <i>Georgia Institute of Technology</i> , Jeong-Geun Kim, <i>Kwangjuon University</i> , Glenn Hopkins, <i>Georgia Tech Research</i>	<b>TU3C-2: A Nonreciprocal, Frequency-Tunable Notch Amplifier Based on Distributedly Modulated Capacitors (DMC)</b> Shihan Qin, <i>Univ. of California, Los Angeles</i> , Yuanxun Ethan Wang, <i>Univ. of California, Los Angeles</i>	<b>TU3D-2: High-Power Continuous-Wave Terahertz Generation Through Plasmonic Photomixers</b> Mona Jarrahi, <i>University of California, Los Angeles</i>
14:10-14:20	<b>TU3A-3: Bandpass Filtering Power Divider with Sharp Roll-Off Skirt and Enhanced In-Band Isolation</b> Wei Jiang, <i>Univ. of South Carolina</i> , Tengxing Wang, <i>Univ. of South Carolina</i> , Yujia Peng, <i>Univ. of South Carolina</i> , Yong Mao Huang, <i>Univ. of Electronic Science &amp; Technology of China</i> , Guoan Wang, <i>Univ. of South Carolina</i>	<b>TU3B-3: A 2.8-to-6 GHz High-Efficiency CMOS Power Amplifier with High-order Harmonic Matching Network</b> Jikang Nai, <i>National Taiwan Univ.</i> , YuanHong Hsiao, <i>National Taiwan Univ.</i> , YuanShan Wang, <i>National Taiwan Univ.</i> , Yu-Hsuan Lin, <i>National Taiwan Univ.</i> , Hwei Wang, <i>National Taiwan Univ.</i>	<b>TU3C-3: Integrated Diversity Front-End for Digital Satellite Radio Reception</b> Juergen Roeber, <i>Univ. of Erlangen-Nuremberg</i> , Simon Senega, <i>Universität der Bundeswehr München</i> , Andreas Baenisch, <i>Infinion Technologies AG</i> , Amelie Hagelauer, <i>Univ. of Erlangen-Nuremberg</i> , Robert Weigel, <i>Univ. of Erlangen-Nuremberg</i> , Stefan Lindenmeier, <i>Universität der Bundeswehr München</i>	<b>TU3D-3: High-Power, Broadband Terahertz Radiation from Large Area Plasmonic Photoconductive Emitters Operating at Telecommunication Optical Wavelengths</b> Nezhiz Yardimci, <i>University of California, Los Angeles</i> , Mona Jarrahi, <i>University of California, Los Angeles</i>
14:20-14:30	<b>TU3A-4: General Model for Loaded Stub Branch-Line Coupler</b> Qiuyi Wu, <i>University of Ontario Institute of Technology</i> , Yimin Yang, <i>University of Waterloo</i> , Ying Wang, <i>University of Ontario Institute of Technology</i> , Xiaowei Shi, <i>Xidian</i>	<b>TU3B-4: Two-way Concurrent Dual-Band Power Amplifier at 0.9/1.8 GHz with Low Second Harmonic and Intermodulation</b> Zhijiang Dai, <i>Univ. of Electronic Science and Tech. of China</i> , Songbai He, <i>Univ. of Electronic Science and Tech. of China</i> , Jingzhou Pang, <i>Univ. of Electronic Science and Tech. of China</i> , Chaoyi Huang, <i>Univ. of Electronic Science and Tech. of China</i> , Tian Qi, <i>Univ. of Electronic Science &amp; Tech. of China</i>		
14:30-14:40	<b>TU3A-5: An N-Way Transformer Based Wilkinson Power Divider in CMOS</b> Fei Wang, <i>Georgia Institute of Technology</i> , Hua Wang, <i>Georgia Institute of Technology</i>	<b>TU3B-5: Measured Linearity Improvement of 10 W GaN HEMT PA with Dynamic Gate Biasing Technique for Flat Transfer Phase</b> Dragan Gecan, <i>Norwegian Univ. of Science and Technology</i> , Morten Olavsbråten, <i>Norwegian Univ. of Science and Technology</i> , Karl Martin Gertsen, <i>Disruptive Technologies Research</i>	<b>TU3C-4: All-Digital Flexible Uplink Remote Radio Head for C-RAN</b> André Prata, <i>Universidade de Aveiro</i> , Amaldo Oliveira, <i>Universidade de Aveiro - DETI / IT - Aveiro</i> , Nuno Carvalho, <i>Instituto de Telecomunicações</i>	<b>TU3D-4: Heterodyne Terahertz Detection with Plasmonic Photomixers</b> Ning Wang, <i>University of California, Los Angeles</i> , Hamid Javaidi, <i>Jet Propulsion Laboratory</i> , Mona Jarrahi, <i>University of California, Los Angeles</i>
14:40-14:50				
14:50-15:00	<b>TU3A-6: Simple Broadband Gysel Combiner with a Single Coupled Line</b> Ali Darwish, <i>Army Research Lab.</i> , Kenneth McKnight, <i>Army Research Lab.</i> , Mona Zaghloul, <i>George Washington University</i> , Edward Viveiros, <i>Army Research Lab.</i> , Alfred Hung, <i>Army Research Lab.</i>		<b>TU3C-5: Design for TV Whitespace Operational Compliance for Cognitive Radio Enabled HighIF WLAN/LTE Front-Ends</b> Arun Ashok, <i>RWTH Aachen Univ.</i> , Iyappan Subbiah, <i>RWTH Aachen University</i> , Gabor Varga, <i>RWTH Aachen University</i> , Moritz Schrey, <i>RWTH Aachen University</i> , Stefan Heinen, <i>RWTH Aachen University</i>	<b>TU3D-5: Fully-Integrated and Electronically-Controlled Millimeter-Wave Beam-Scanning</b> Mohammed Reza Hashemi, <i>Univ. of California, Los Angeles</i> , ShangHua Yang, <i>Univ. of California, Los Angeles</i> , Tongyu Wang, <i>Michigan State Univ.</i> , Nelson Sepúlveda, <i>Michigan State Univ.</i> , Mona Jarrahi, <i>Univ. of California, Los Angeles</i>
15:00-15:10	<b>TU3A-7: A Design of Negative Group Delay Power Divider: Coupling Matrix Approach with Finite Unloaded-Qu Resonators</b> Girdhari Chaudhary, <i>Chonbuk National Univ.</i> , Phirun Kim, <i>Chonbuk National Univ.</i> , Junhyung Jeong, <i>Chonbuk National Univ.</i> , Yongchae Jeong, <i>Chonbuk National Univ.</i>			<b>TU3D-6: Metamaterial Modulators for Terahertz Communications and Coded Aperture Imaging</b> Willie Padilla, <i>Duke University</i>

# Tuesday

# Technical Sessions

13:30-15:10

	Room: 307	Room: 308	Room:309
	<b>TU3E: Signal Generation Techniques For Radar and Communication Systems</b> Chair: Deukhyoun Heo, <i>Washington State Univ.</i> Co-Chair: Brad Nelson, <i>QORVO, Inc.</i>	<b>TU3F: Novel Planar and Lumped-Element Filtering Devices</b> Chair: Shamsur Mazymder, <i>Raytheon Company</i> Co-Chair: Roberto Gomez-Garcia, <i>Univ. of Alcalá</i>	<b>TU3G: Green, Flexible, Wearable, Reconfigurable Technologies</b> Chair: Zaher Bardai, <i>IMN Epiphany</i> Co-Chair: Ramesh Gupta, <i>LightSquared</i>
13:30-13:50	<b>TU3E-1: A 10 GHz Phase Noise Filter with 10.6 dB Phase Noise Suppression and -116 dBc/Hz Sensitivity at 1 MHz Offset</b> Shilei Hao, <i>University of California, Davis</i> , Jane Gu, <i>University of California, Davis</i>	<b>TU3F-1: Power-Dependent Bandstop Filters for Frequency-Selective Limiting</b> Eric Naglich, <i>Naval Research Laboratory</i> , Andrew Guyette, <i>Naval Research Laboratory</i>	<b>TU3G-1: Efficiency Enhancement Solutions for an Original Linear Green RF Transmitters</b> Nathalie Deltimple, <i>University of Bordeaux</i> , Guillaume Ferré, <i>University of Bordeaux</i> , Mouna Ben Mabrouk, <i>University of Bordeaux</i> , Eric Kerhervé, <i>University of Bordeaux</i>
13:50-14:10	<b>TU3E-2: A Fully-Integrated Digitally-Programmable 4x4 Picosecond Digital-to-Impulse Radiating Array in 65nm Bulk CMOS</b> M. Mahdi Assefzadeh, <i>Rice University</i> , Aydin Babakhani, <i>Rice University</i>	<b>TU3F-2: Tunable Acoustic-Wave-Lumped-Element Resonator (AWLR)-Based Band-Pass Filters</b> Dimitra Psychogiou, <i>Purdue University</i> , Roberto Gomez-Garcia, <i>University of Alcalá</i> , Dimitrios Peroulis, <i>Purdue University</i>	<b>TU3G-2: Green Microwave Electronics for the Coming Era of Flexible Electronics</b> Zhenqiang Ma, <i>University of Wisconsin</i> , Yei Hwan Jung, <i>University of Wisconsin</i> , Tzu-Hsuan Chang, <i>University of Wisconsin</i> , Jung-Hun Seo, <i>University of Wisconsin</i> , Huilong Zhang, <i>University of Wisconsin</i> , Zhiyong Cai, <i>USDA Forrest Products Laboratory</i> , Shaoqin Gong, <i>University of Wisconsin</i>
14:10-14:20	<b>TU3E-3: A 65nm CMOS 88-105 GHz DDFS-Based Fractional Synthesizer For High Resolution Planetary Exploration Spectroscopy</b> Adrian Tang, <i>Jet Propulsion Laboratory</i> , Theodore Reck, <i>Jet Propulsion Laboratory</i> , Yangyho Kim, <i>University of California, Los Angeles</i> , Gabriel Virbila, <i>University of California, Los Angeles</i> , Goutam Chattopadhyay, <i>Jet Propulsion Laboratory</i> , Mau-Chung Chang, <i>University of California, Los Angeles</i>	<b>TU3F-3: A Compact 1.9-3.4GHz Diplexer with Controllable Transmission Zeros, Improved Isolation, and Constant Fractional Bandwidth</b> Tao Yang, <i>University of California at San Diego</i> , Gabriel Rebeiz, <i>University of California at San Diego</i>	<b>TU3G-3: Investigation of Microwave Active Elements Embedded in Composite Structures</b> Thomas Baum, <i>RMIT University</i> , Richard Ziolkowski, <i>University of Arizona</i> , Kelvin Nicholson, <i>DST Group</i> , Richard Ziolkowski, <i>University of Arizona</i>
14:30-14:40	<b>TU3E-4: A K-Band Low Phase Noise and High Gain Gm Boosted Colpitts VCO for 76 – 81 GHz FMCW Radar Applications</b> Run Levinger, <i>IBM Research - Haifa</i> , Roe Ben Yishay, <i>IBM Research - Haifa</i> , Jakob Vovnoy, <i>IBM Research - Haifa</i> , Oded Katz, <i>IBM Research - Haifa</i> , Danny Elad, <i>IBM Research - Haifa</i>	<b>TU3F-4: A Class of Fully-Reconfigurable Planar Multi-Band Bandstop Filters</b> Dimitra Psychogiou, <i>Purdue University</i> , Roberto Gomez-Garcia, <i>University of Alcalá</i> , Dimitrios Peroulis, <i>Purdue University</i>	<b>TU3G-4: Electrically Tunable Bandpass Filtering Balun on Engineered Substrate Embedded with Patterned Permalloy Thin Film</b> Yujia Peng, <i>University of South Carolina</i> , Yong Mao Huang, <i>University of Electronic Science &amp; Technology of China</i> , Tengxing Wang, <i>University of South Carolina</i> , Wei Jiang, <i>University of South Carolina</i> , Guoan Wang, <i>University of South Carolina</i>
14:40-14:50			
14:50-15:00	<b>TU3E-5: A 5.8 GHz and -192.9 dBc/Hz FoMT CMOS Class-B Capacitively-Coupled VCO with Gm-Enhancement</b> Tai Nguyen, <i>Washington State University</i> , Pawan Agarwal, <i>Washington State University</i> , Deukhyoun Heo, <i>Washington State University</i>	<b>TU3F-5: Multi-Functional Low-Pass Filters With Dynamically-Controlled In-Band Rejection Notches</b> Dimitra Psychogiou, <i>Purdue University</i> , Roberto Gomez-Garcia, <i>University of Alcalá</i> , Dimitrios Peroulis, <i>Purdue University</i>	
15:00-15:10			

# A Design of Negative Group Delay Power Divider: Coupling Matrix Approach with Finite Unloaded- $Q_u$ Resonators

Girdhari Chaudhary, Phirun Kim, Junhyung Jeong and Yongchae Jeong

Division of Electronics and Information Engineering, Chonbuk National University, Jeonju, Korea

**Abstract** — In this paper, a novel approach to design a power divider with the predefined negative group delay (NGD) is presented. The proposed topology is based on a coupling matrix with a finite unloaded quality factor ( $Q_u$ ) of resonators, which does not require any lumped elements such as resistor for generating NGD. The NGD bandwidth and magnitude flatness can be controlled by inter-resonating couplings. As an experimental illustration, a microstrip line NGD power divider is designed and fabricated at center frequency of 2.14 GHz. The measurement results are in good agreement with simulations.

**Index Terms** — Delay lines, negative group delay, power divider, pre-distortion amplifier.

## I. INTRODUCTION

A propagation of electromagnetic waves in dispersive media can lead to interesting phenomena including abnormal negative group velocities (NGVs) and negative group delays (NGDs) [1]. When an electromagnetic wave traverses in such dispersive material or electronic circuit, the peak of a pulse envelope emerges from a medium at an instant before a peak of pulse enters. However, this phenomena does not violate Einstein's causality, because turn on and off points of the wave packet propagate with a positive delay in an agreement with the causality requirement. The structures that support a propagation with the NGD have been theoretically and experimentally studied at microwave frequencies and applied in various applications such as realizing non-Foster reactive elements [2], [3].

In microwave circuits and systems, power dividers are widely adopted such as a feeding network in antenna arrays and power divider/combiner in power amplifiers [4], [5]. Modern RF wireless communication systems require highly linear high power amplifiers because of complex modulation techniques to handle higher data rate transmissions. A predistortion is one of the low cost linearization techniques, which have advantages of low-power consumption and simple circuit configuration [5]. In this technique, it is crucial to match group delay (GD), magnitude, and phase of different paths in the predistortion circuit for a linearity enhancement. Therefore, if a research that can demonstrate the power divider with the NGD would be promising for the predistortion amplifier for compensating a positive delay that can eliminate the delay element and attenuator. In [6], the power divider with the NGD is presented, but this structure suffers from a narrow NGD bandwidth (which is defined as a bandwidth when  $GD < 0$ ) and poor magnitude flatness.

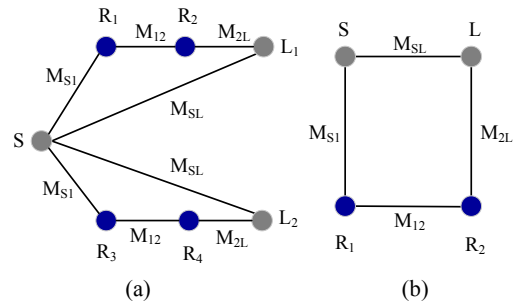


Fig. 1. (a) Topology of the proposed power divider and (b) even-mode equivalent topology.

In this paper, the NGD power divider is presented based on a coupling matrix approach, which provides a wider bandwidth and excellent magnitude flatness.

## II. DESIGN THEORY

The topology of the proposed power divider is shown in Fig. 1(a), where  $R_1$ - $R_4$  represent four lossy resonators and  $S$ ,  $L_1$ , and  $L_2$  denote three ports. Since the structure is symmetrical, even- and odd-mode analysis can be applied to find the  $S$ -parameters, which is expressed as [4].

$$[S] = \begin{bmatrix} S_{11e} & \frac{S_{21e}}{\sqrt{2}} & \frac{S_{21e}}{\sqrt{2}} \\ \frac{S_{21e}}{\sqrt{2}} & \frac{S_{22e} + S_{22o}}{2} & \frac{S_{22e} - S_{22o}}{2} \\ \frac{S_{21e}}{\sqrt{2}} & \frac{S_{22e} - S_{22o}}{2} & \frac{S_{22e} + S_{22o}}{2} \end{bmatrix} \quad (1)$$

where  $S_{11e}$ ,  $S_{22e}$ ,  $S_{21e}$ , and  $S_{22o}$  are  $S$ -parameters of even- and odd-mode equivalent sub-circuits, respectively.

Fig. 1(b) shows the even-mode equivalent topology under the even-mode excitation, which is equivalent to a second-order filter with source-load and inter-resonating couplings. Therefore,  $(N+2) \times (N+2)$  coupling matrix of equivalent even-mode sub-circuit can be expressed as [7].

$$M_e = \begin{bmatrix} 0 & M_{S1} & 0 & M_{SL} \\ M_{S1} & M_{11} & M_{12} & 0 \\ 0 & M_{12} & M_{22} & M_{2L} \\ M_{SL} & 0 & M_{2L} & 0 \end{bmatrix} \quad (2)$$

For a finite unloaded quality factor  $Q_u$  and 3-dB fractional bandwidth  $\Delta$ , self-coupling values of lossy resonators are given as below [7].

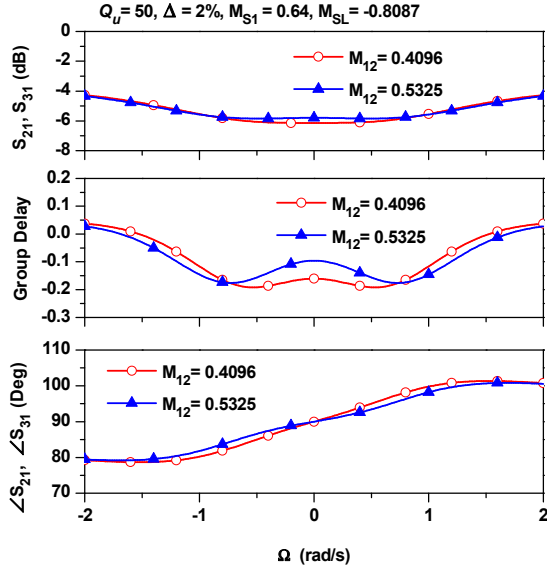


Fig. 2. Synthesized results of the proposed power divider with different values of  $M_{12}$ .

$$M_{11} = M_{22} = -\frac{j}{Q_u \Delta} \quad (3)$$

Assuming  $M_{S1} = M_{2L}$ , the transmission coefficients of the proposed power divider are expressed as (4).

$$S_{21} = S_{31} = \frac{2M_{SL} \Omega + j \left( M_{SL} \Omega^2 + M_{S1}^2 M_{12} - M_{SL} M_{12}^2 - \frac{M_{SL}}{Q_u^2 \Delta^2} \right)}{\left[ \frac{M_{S1}^4}{2} + \frac{(M_{SL}^2 + 1) M_{12}^2}{2} - \frac{(M_{SL}^2 + 1)}{2} \Omega^2 \right.} \quad (4)$$

$$\left. + \sqrt{2} \left\{ \frac{M_{S1}^2}{Q_u \Delta} + \frac{(M_{SL}^2 + 1)}{2 Q_u^2 \Delta^2} - M_{S1}^2 M_{12} M_{SL} \right\} \right. \\ \left. + j \left( M_{S1}^2 + \frac{M_{SL}^2 + 1}{Q_u \Delta} \right) \Omega \right]$$

And GDs of different transmission paths can be found as (5).

$$\tau_{21} = \tau_{31} = -\frac{d \angle S_{21}}{d \Omega} = -\frac{d \angle S_{31}}{d \Omega} \quad (5)$$

Based on above design equations, the synthesized results are plotted in Fig. 2 and 3. As observed from Fig. 2, the magnitude flatness as well as NGD bandwidth are controlled by the inter-resonator coupling of resonators. For a wider NGD bandwidth, a strong coupling between resonators is preferable. However, it may decrease overall GD value. Similarly, the GD and magnitude are also controlled by unloaded quality factor  $Q_u$  of resonators as shown in Fig. 3. When the value of  $Q_u$  increases from 50 to 60, magnitudes of  $S_{21}$  (insertion loss) and NGD are also increased. However, the low value  $Q_u$  is preferable for a low insertion loss.

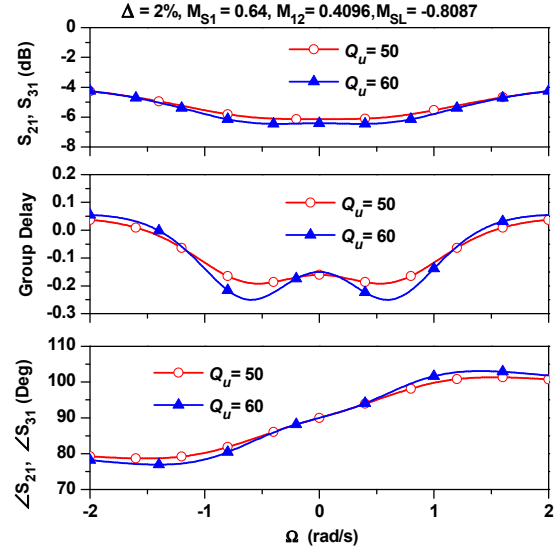


Fig. 3. Synthesized results of the proposed power divider with different values of  $Q_u$ .

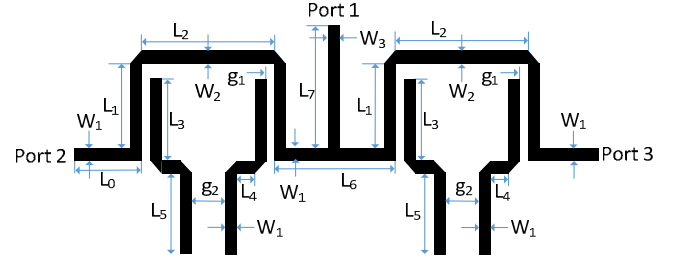


Fig. 4. EM simulation layout with physical dimensions:  $W_1 = 1.8$ ,  $W_2 = 3.7$ ,  $W_3 = 2.7$ ,  $L_0 = 8.2$ ,  $L_1 = 12.3$ ,  $L_2 = 17.4$ ,  $L_3 = 14.1$ ,  $L_4 = 1.5$ ,  $L_5 = 20$ ,  $L_6 = 19.1$ ,  $L_7 = 20.2$ ,  $g_1 = 0.6$ ,  $g_2 = 6$ . (Unit: mm).

### III. SIMULATION AND MEASUREMENT RESULTS

For an experimental demonstration, the power divider with the GD of  $-0.5$  ns is designed and fabricated at a center frequency of  $2.14$  GHz. The circuit is fabricated on FR-4 epoxy substrate with a dielectric constant of  $4.4$ , thickness of  $0.787$ , and loss tangent of  $0.02$ . The physical dimensions of the fabricated circuit are optimized using ANSYS HFSS 15.

The resonators are implemented with open-circuited  $\lambda/2$  transmission line and coupling between source and load with  $3\lambda/4$  line. Using HFSS Eigen-mode simulation,  $Q_u$  of the  $\lambda/2$  resonator in the FR-4 epoxy substrate is estimated as  $50$ . The coupling matrix is extracted for the given specification of power divider as  $M_{S1} = 0.69$ ,  $M_{12} = 0.3468$ , and  $M_{SL} = -0.7677$  with  $Q_u = 50$  and  $\Delta = 2\%$ . The electromagnetic (EM) simulation layout of the designed NGD power divider is shown in Fig. 4 with physical dimensions. A  $\lambda/4$  impedance transformer is used to match an input port.

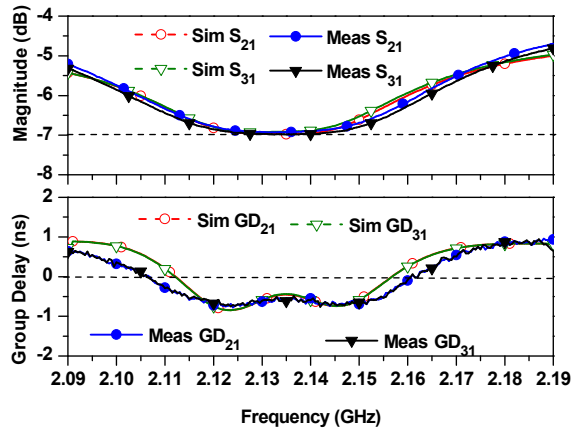


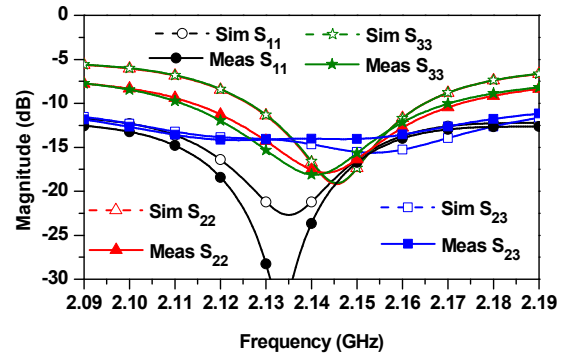
Fig. 5. Simulated and measured magnitude and group delay of the proposed power divider.

The simulated and measured GDs and magnitudes are shown in Fig. 5. From the measurement, the insertion losses are  $|S_{21}| = -6.95$  dB and  $|S_{31}| = -6.97$  dB, while the GDs are  $\tau_{21} = -0.54$  ns and  $\tau_{31} = -0.56$  ns at  $f_0 = 2.138$  GHz. Due to the tradeoff between maximum achievable NGD, insertion loss, and BW, the appropriate parameter to compare performances of circuits is a NGD-BW product. Therefore, the NGD-BW products for the different transmission paths are determined as 0.034 and 0.0336, respectively.

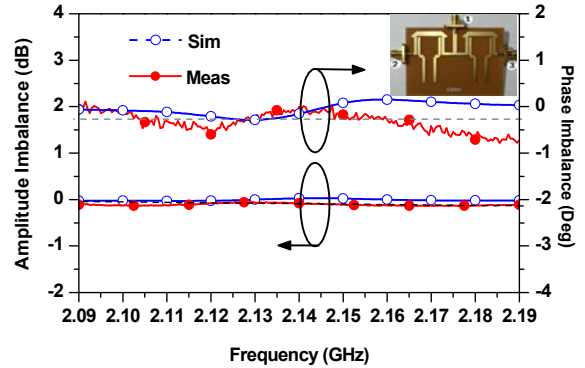
The simulated and measured return loss and isolation characteristics are shown in Fig. 6(a). From the experiment, the return losses are determined as  $|S_{11}| = -28.9$  dB,  $|S_{22}| = -17.5$  dB, and  $|S_{33}| = -18.2$  dB at  $f_0$ . The measured isolation ( $|S_{23}|$ ) at  $f_0$  is -15.8 dB. The measured amplitude imbalance and phase differences between the two output ports are shown in Fig. 6(b). It can be seen that the maximum amplitude imbalance of  $\pm 0.1$  dB and the phase imbalance of  $\pm 0.6^\circ$  are observed over the bandwidth of 100 MHz.

#### IV. CONCLUSION

A negative group delay power divider is proposed, investigated, and fabricated in this paper. The proposed power divider is analyzed and designed based a coupling matrix approach with finite unloaded  $Q_i$  resonators. The simulated and measured results show negative group delay, good return, and high isolation characteristics. The proposed power divider is promising for compensating group delay mismatch between direct and inter-modulation generation paths of predistortion amplifier, which can eliminate the delay element. In addition, this circuit can be also employed as a feeding network of series-fed antenna arrays for a performance improvement by compensating group delay and minimizing beam-squint problem.



(a)



(b)

Fig. 6. Simulated and measurement results of the proposed power divider: (a) return losses/isolation and (b) amplitude/phase imbalances.

#### REFERENCES

- [1] L. Brillouin, *Wave propagation and group velocity*, Academic Press, New York, NY, 1960.
- [2] S. Gharavi and M. Mojahedi, "Theory and application of gain-assisted periodically loaded transmission lines with negative or superluminal group delays," *Antennas and Propagation Society International Symposium (APSURSI)*, pp. 2373-2376, Jun. 2007.
- [3] H. Mirzaei and G. V. Eleftheriades, "Arbitrary-angle squint-free beamforming in series-fed antenna arrays using non-Foster elements synthesized by negative group delay networks," *IEEE Trans. Antenna and Propagation*, vol. 63, no. 5, pp. 1997-2010, May 2015.
- [4] H. R. Ahn, *Asymmetric passive components in Microwave Integrated Circuits*, New York, NY, USA: Wiley, 2006.
- [5] J. Yi, Y. Yang, M. Park, W. Kang, and B. Kim, "Analog predistortion linearizer for high power RF amplifiers," *IEEE Trans. Microw. Theory Tech.*, vol. 48, no. 12, pp. 2709-2913, Dec. 2000.
- [6] G. Chaudhary and Y. Jeong, "A design of power divider with negative group delay characteristics," *IEEE Microw. Wireless Compon. Letters*, vol. 25, no. 6, pp. 394-396, Jun. 2015.
- [7] E. J. Naglich, J. Lee, D. Peroulis, and W. J. Chappell, "Switchless tunable bandstop to all-pass reconfigurable filter," *IEEE Trans. Microw. Theory Tech.*, vol. 60, no. 5, pp. 1258-1265, May 2012.